Size and Composition Dependent Multiple Exciton Generation Efficiency in PbS, PbSe, and PbSxSe1−x Alloyed Quantum Dots

ARTICLE *in* NANO LETTERS · JUNE 2013

Impact Factor: 13.59 · DOI: 10.1021/nl4009748 · Source: PubMed

8 AUTHORS, INCLUDING:

Aaron G Midgett
University of Colorado Boulder
13 PUBLICATIONS **593** CITATIONS
SEE PROFILE

Joseph M Luther
National Renewable Energy Laboratory
83 PUBLICATIONS **5,233** CITATIONS
SEE PROFILE

A. J. Nozik
University of Colorado Boulder
310 PUBLICATIONS **19,397** CITATIONS
SEE PROFILE

Matthew C Beard
National Renewable Energy Laboratory
113 PUBLICATIONS **7,860** CITATIONS
SEE PROFILE

NANO LETTERS

Letter

pubs.acs.org/NanoLett

Size and Composition Dependent Multiple Exciton Generation Efficiency in PbS, PbSe, and PbS_xSe_{1-x} Alloyed Quantum Dots

Aaron G. Midgett,[†,‡] Joseph M. Luther,[†] John T. Stewart,[§] Danielle K. Smith,[†] Lazaro A. Padilha,[§] Victor I. Klimov,[§] Arthur J. Nozik,[†,‡] and Matthew C. Beard*[,†]

[†]National Renewable Energy Laboratory, Golden, Colorado 80401, United States

[‡]Chemistry and Biochemistry Department, University of Colorado, Boulder, Colorado 80309, United States

[§]Center for Advanced Solar Photophysics, Los Alamos National Laboratory, Los Alamos, New Mexico 87545, United States

ABSTRACT: Using ultrafast transient absorption and time-resolved photoluminescence spectroscopies, we studied multiple exciton generation (MEG) in quantum dots (QDs) consisting of either PbSe, PbS, or a PbS_xSe_{1-x} alloy for various QD diameters with corresponding bandgaps (E_g) ranging from 0.6 to 1 eV. For each QD sample, we determine the MEG efficiency, η_{MEG}, defined in terms of the electron–hole pair creation energy (ε_{eh}) such that $\eta_{MEG} = E_g/\varepsilon_{eh}$. In previous reports, we found that η_{MEG} is about two times greater in PbSe QDs compared to bulk PbSe, however, little could be said about the QD-size dependence of MEG. In this study, we find for both PbS and PbS_xSe_{1-x} alloyed QDs that η_{MEG} decreases lineally with increasing QD diameter within the strong confinement regime. When the QD radius is normalized by a material-dependent characteristic radius, defined as the radius at which the electron–hole Coulomb and confinement energies are equivalent, PbSe, PbS, and PbS_xSe_{1-x} exhibit similar MEG behaviors. Our results suggest that MEG increases with quantum confinement, and we discuss the interplay between a size-dependent MEG rate versus hot exciton cooling.

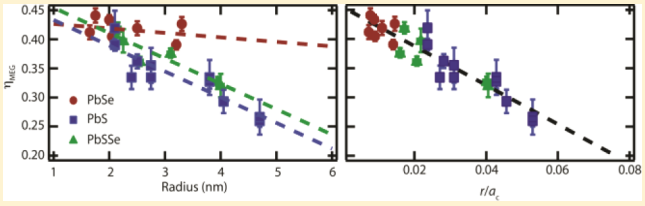

KEYWORDS: *Multiple exciton generation, carrier multiplication, quantum size effects, solar energy conversion, exciton dynamics, PbS quantum dots*

Multiple exciton generation (MEG) or carrier multiplication (CM) from a single high-energy photon has been observed in several quantum dot (QD) systems with the lead chalcogenide QDs (PbX; X = S, Se, Te) being the most studied.[1−9] For MEG studies, PbX offers several unique advantages such as small bulk bandgap (with large range of tunability using quantum confinement), large Bohr exciton radius (a_B = 46 nm in PbSe; 18−20 nm in PbS; and ∼80 nm in PbTe),[10,11] good stability, and relatively well-established and reproducible synthesis. Furthermore, PbX QDs are promising for solar applications due to their natural abundance,[12] ease of processing, large carrier mobilities, and low exciton binding energies that simplify electron–hole separation following photogeneration of an exciton. Enhanced MEG in QDs could allow for surpassing the Shockley–Queisser (SQ) limit for solar energy conversion.[13] As a proof-of-principle, we recently demonstrated the first solar cells with external quantum efficiency (EQE) greater than 100%.[14] Those solar cells employed PbSe QDs as the active (light-absorbing) medium and when the internal quantum efficiency (IQE) is compared to recent spectroscopic measurements of MEG[15,16] we find excellent agreement, providing confidence in the QYs extracted from ultrafast spectroscopic studies. There have been other measurements within device structures employing quantum-confined nanoparticles that also indicate MEG. Sambur et al. observed internal quantum efficiencies (IQE) greater than 100% for single monolayer of PbS QDs that were strongly coupled to an atomically flat TiO_2 anatase surface.[17] Hints of multiple carrier collection were observed in biased IQE measurements of a PbS QD photodiode structure.[18,19] These device measurements provide incentive to better understand MEG in isolated QDs[8,20] as well as electronically coupled arrays of QDs.[21]

When viewed in terms of the relevant physics involved, the amount of excess energy needed to produce an extra electron–hole (e-h) pair, and/or the competition between an MEG relaxation pathway and hot-exciton cooling via heat dissipation, we argue that PbSe QDs are about 2−3 times better than bulk PbSe in producing multiple excitons.[55] In our view, to properly assess how efficient the MEG process is for a set of materials with different bandgaps it is not enough to simply compare the QYs at particular photon energies.[3,22,23] While the QY at particular photon energy measures the number of e-h pairs produced, it does not consider the excess energy available for producing extra carriers. There are two characteristics of the MEG process that are generally reported: (1) the MEG threshold, $h\nu_{th}$, which is the photon energy at which the QYs begin to exceed 1, and (2) the electron–hole pair creation energy, ε_{eh},[4,24] which is the required excess energy to produce

Received: March 15, 2013
Revised: May 30, 2013
Published: June 10, 2013

   dx.doi.org/10.1021/nl4009748 | *Nano Lett.* 2013, 13, 3078−3085

one additional e-h pair, $\varepsilon_{eh} = \Delta h\nu/\Delta QY$, for $h\nu > h\nu_{th}$. The analysis of a large body of experimental data suggests[5] that these two characteristics can be directly related by $h\nu_{th} = E_g + \varepsilon_{eh}$ in the limit of $h\nu_{th} \gtrsim 2.2E_g$. It is convenient to express the e-h pair creation energy in terms of E_g and the dimensionless MEG efficiency, η_{MEG}: $\varepsilon_{eh} = E_g/\eta_{MEG}$[5] and thus $h\nu_{th} = E_g(1 + 1/\eta_{MEG})$. The η_{MEG} serves as a photon-energy-independent measure of MEG and captures the underlying photophysics regarding the competition between a hot carrier cooling to the band edge and the processes leading to production of new electron−hole pairs. If the enhanced QYs are compared on an absolute photon energy ($h\nu$) basis, results obtained from bulk PbSe are in many cases higher than that for QDs.[23] The reason for this is that the bandgap energy is much lower in bulk PbSe (0.27 eV) compared to PbSe QDs (0.6−2.0 eV), such that the amount of excess energy for example in a 4 eV photon is well above the e-h creation energy for bulk PbSe, but not for a large bandgap PbSe QD. Therefore, to directly assess the MEG efficiency, it is more informative to plot the enhanced QYs on a $h\nu/E_g$ basis as will be demonstrated below.

Despite the enhanced MEG in PbSe QDs over bulk PbSe, further improvements are necessary to have a meaningful impact on solar energy conversion technologies. For PbSe QDs, extra e-h pairs are produced when the photon energy exceeds ~2.8−3.0 E_g and reaches 2 e-h pairs at ~6 E_g. These characteristics are captured by a η_{MEG} between 0.4 and 0.5. A major research challenge is to gain a better understanding of the factors that govern MEG so as to design systems that can maximize its efficiency. An ideal MEG material could produce 2 e-h pairs at $2E_g$, 3 at $3E_g$, and so forth. There are recent reports that have demonstrated more efficient MEG than has been found in PbSe QDs. For example, quantum rods (QRs) of PbSe appear to be ~1.5× as efficient as QDs.[25,26] Si QDs (both colloidal[27] and embedded in a matrix such that the QDs are electronically coupled[28]) display η_{MEG} approaching the ideal limit. Other promising nanomaterials include CNTs,[29] and III−V QD[30] systems. Here, we show within the PbSe and PbS system how MEG depends on the degree of quantum confinement.

There are two factors that influence η_{MEG}: the rate of producing multiexcitons from the initially photogenerated hot-exciton, k_{MEG}, and the competition with hot-exciton cooling pathways, k_{cool}. The enhanced QY can be expressed in terms of the rate constants for MEG and cooling, k_{MEG}, and k_{cool}, by[5]

$$QY = 1 + \frac{k_{MEG}^{(1)}}{(k_{MEG}^{(1)} + k_{cool})} + \frac{k_{MEG}^{(1)}k_{MEG}^{(2)}}{(k_{MEG}^{(1)} + k_{cool})(k_{MEG}^{(2)} + k_{cool})} + \cdots \quad (1)$$

where $k_{MEG}^{(i)}$ is the rate constant for producing $(i + 1)$ excitons from (i) hot excitons. In deriving eq 1, we assume that k_{cool} of single- and multiexcitons are equivalent and that k_{MEG} only depends on the initial excess energy supplied by the photon. Note that each successive term in eq 1 is only valid when energy conservation applies, thus when the photon energy is greater than $3E_g$ the three terms can all contribute ($k_{MEG}^{(i)}$ is zero when the photon energy is less than $(i + 1)E_g$). When $h\nu > 3E_g$ higher order terms can be included by expanding the series.

In principle, both $k_{MEG}^{(i)}$ and k_{cool} could be dependent on the amount of excess photon energy. In bulk semiconductors, the rate of carrier cooling, k_{cool}, has been shown to be relatively independent of excess energy,[31] while k_{MEG} increases rapidly above $h\nu_{th}$.[32,33] Assuming that k_{cool} also does not increase significantly with excess photon energy in QDs[34] then k_{MEG} and k_{cool} are related by[35]

$$k_{MEG} = Pk_{cool}\left(\frac{h\nu_{ex}}{h\nu_{th}}\right)^s \quad (2)$$

where $h\nu_{ex} = h\nu - h\nu_{th}$, and P describes the competition between k_{MEG} and k_{cool} such that at a photon energy $h\nu = 2h\nu_{th}$ $_{ex} = h\nu_{th}$, and thus $k_{MEG} = Pk_{cool}$, (note that when $h\nu < h\nu_{th}$, k_{MEG} = 0). The exponent s is related to how k_{MEG} changes with increasing excess energy and is typically found to be between 2 and 5. For example, a recent theoretical treatment found s to be between 2.1 and 2.6 for CdSe QDs.[36] Here we find s to be ~2.2. Thus the number of e-h produced and $h\nu_{th}$ are related and will both improve if k_{MEG}/k_{cool} is increased. To compare the QY results for different samples, we determine MEG efficiency, η_{MEG}, and P.

We studied PbS and PbS_xSe_{1-x} QDs with bandgaps ranging from 0.6 to 1 eV (see Figure 1 for absorption spectra) and

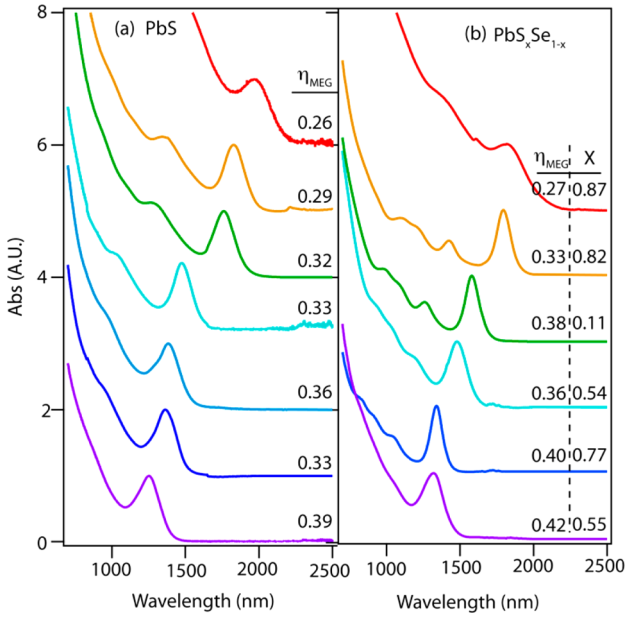

Figure 1. Absorbance data are shown for (a) PbS samples along with the MEG efficiency (η_{MEG}) and (b) PbS_xSe_{1-x} alloy samples with η_{MEG} and x.

compare the results to previous studies of PbSe QDs. In Figure 2, we display the QYs for PbSe QDs, while Figure 3 shows the QYs for PbS_xSe_{1-x} (top row) and PbS QDs (bottom row). Four PbS samples were synthesized at National Renewable Energy Laboratory (NREL), but analyzed at Los Alamos National Laboratory (LANL), and several PbSe QD samples were studied at Delft University of Technology and are reported in ref 8 For the smallest size of PbS (E_g = 0.99 eV and d = 4.2 nm) the QY is very similar to that found for PbSe QDs, however, for the d = 7.6, 8.1, and 9.4 nm samples, the QY is considerably lower for similar excess photoexcitation energies. The largest PbS sample, d = 9.4 nm, has similar QYs as those reported for bulk PbS.[23]

For the alloyed samples, the d = 4.3 nm QDs have about the same QY as the PbSe samples. However, for the d = 5.1, 6.2, 7.9, and 8.0 nm samples, the QYs are much closer to those of

dx.doi.org/10.1021/nl4009748 | Nano Lett. 2013, 13, 3078−3085

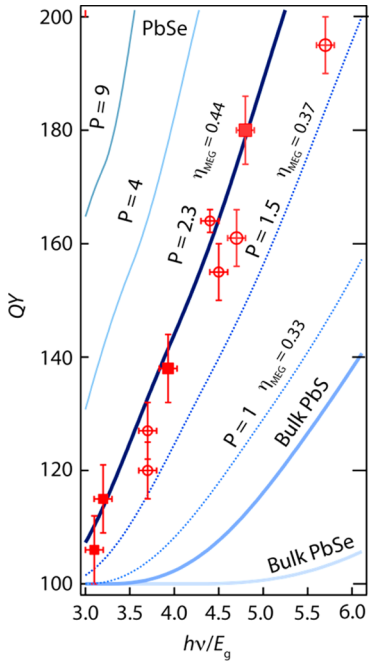

Figure 2. The QYs determined for a variety of sizes of PbSe QDs previously reported. The lines represents various values of η_{MEG}.

PbS QDs than of PbSe QDs. This is particularly interesting for the 6.2 nm $PbS_{11}Se_{89}$ sample, which contains only 11% sulfur: while a similar size PbSe sample shows QY of 161% the QY of the alloyed sample is 140%.

All of the PbSe QD samples studied have similar η_{MEG}'s, (see Figure 2) and tend to fall along the P = 2.3 line (η_{MEG} = 0.4 (shown as the thick blue line) and the optical results are consistent among at least three independent laboratories,[8,9,15,16] as well as with the photocurrent measurements on solar cells.[14] For comparison we plot P = 9, 4, 1.5, and 1.0 and also display the lines that were determined for bulk PbS (η_{MEG} = 0.29; P = 0.83) and bulk PbSe (η_{MEG} = 0.19; P = 0.45) using the data from ref 23. In contrast to PbSe QDs, we find a size-dependent η_{MEG} for PbSSe QDs (Figure 3 top row) and PbS QD (Figure 3 bottom row) samples where the efficiency decreases with increasing QD diameter. In each panel the dark blue line represents the PbSe QD results from Figure 2 while the light blue line is for bulk PbS. The dashed lines are the best-fit lines (using eq 1 and 2) to the results from different sized PbS QDs (the size of QD for each line is noted in each panel). The largest size PbS QD (d = 9.2 nm) has a η_{MEG} that is similar to the reported values for bulk PbS, while the smallest size is similar to that of the PbSe QDs.

In Table 1, we tabulate our findings along with QD diameter (calculated from sizing curves and verified with TEM), bandgaps, percentages of sulfur and selenium, QY at a given $h\nu/E_g$, and η_{MEG} of each sample.

In Figure 4a, we plot the extracted η_{MEG} versus QD diameter for PbSe, PbS, and PbS_xSe_{1-x}. As discussed above, η_{MEG} is relatively size-independent for the PbSe QDs, but for PbS and

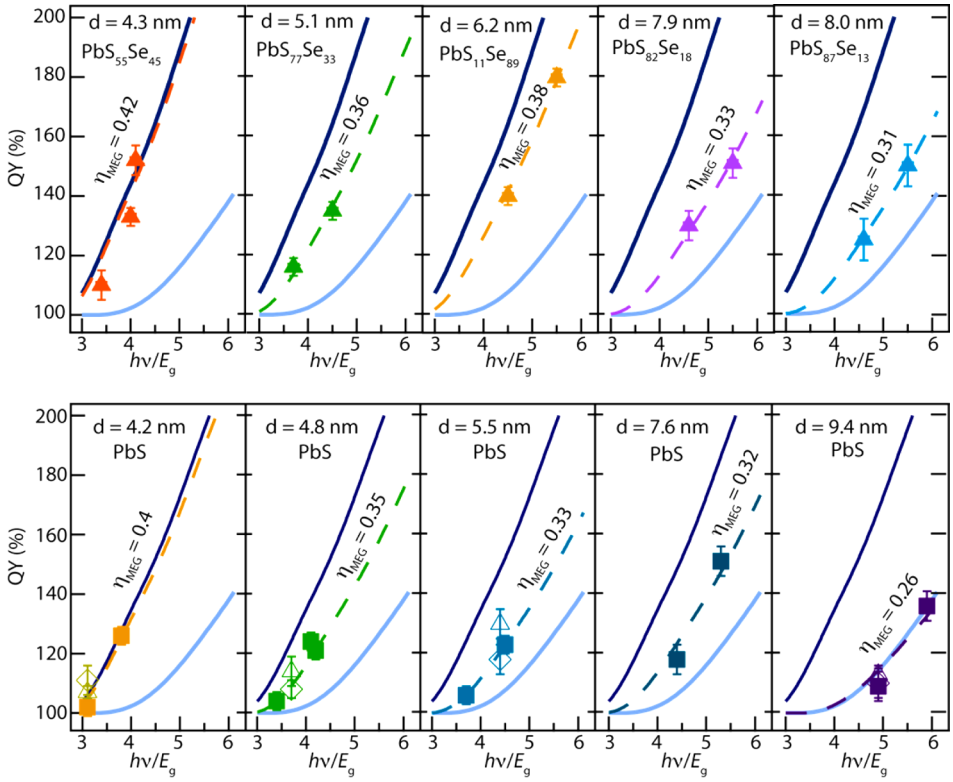

Figure 3. Top row: Photon-to-exciton QYs for various sizes of PbS_xSe_{1-x} alloy QDs determined in this study plotted verses the photon energy relative to the bandgap of the material. Bottom row: QYs for a variety of PbS QD sizes. The filled squares and traingles are from TA measurements performed at NREL while the open diamonds are the open triangles are respectively TA and transient PL measurements at LANL . The solid dark blue line represents η_{MEG} determined from PbSe QDs (see Figure 2) while the light blue lines are for bulk PbS. The dotted lines are η_{MEG} determined from a linear least-squares best-fit to the data of the model discussed in the text. Note that for each size the QY was also determined at $h\nu/E_g$ less than 2 (but not shown).

dx.doi.org/10.1021/nl4009748 | *Nano Lett.* 2013, 13, 3078−3085

Table 1. MEG Data for PbSe, PbS, PbS_xSe_{1-x} Samples Studied[a]

sample	radius (nm)	E_g (eV)	QY (±STD)	$h\nu/E_g$	η_{MEG}
PbSe	2.05	0.89	1.20 (0.05)	3.7	0.41
			1.55 (0.05)	4.5	
	2.0	0.91	1.27 (0.05)	3.7	0.43
			1.64 (0.02)	4.4	
	3.2	0.66	1.61 (0.05)	4.7	0.40
			1.95 (0.05)	5.7	
PbS	2.1	0.99	1.02 (0.02)	3.1	0.40
			1.26 (0.03)	3.8	
	2.4	0.91	1.04 (0.02)	3.4	0.33
			1.21 (0.03)	4.2	
	2.5	0.90	1.24 (0.03)	4.1	0.37
	2.75	0.84	1.06 (0.02)	3.7	0.33
			1.23 (0.03)	4.5	
	3.8	0.70	1.18 (0.03)	4.4	0.32
			1.51 (0.03)	5.3	
	4.05	0.68	1.18 (0.03)	4.6	0.29
	4.7	0.64	1.09 (0.03)	4.9	0.26
			1.36 (0.08)	5.9	
PbS_xSe_{1-x}	2.15	0.93	1.10 (0.02)	3.4	0.42
x = 0.55			1.52 (0.03)	4.1	
x = 0.77	2.25	0.93	1.33 (0.03)	4.0	0.40
x = 0.54	2.55	0.84	1.14 (0.03)	3.7	0.36
			1.35 (0.03)	4.5	
x = 0.11	3.1	0.69	1.40 (0.03)	4.5	0.38
			1.80 (0.03)	5.5	
x = 0.82	3.95	0.68	1.30 (0.03)	4.6	0.33
			1.51 (0.05)	5.5	
x = 0.87	4.0	0.68	125 (0.05)	4.6	0.31
			150 (0.08)	5.5	

[a]List of samples studied at NREL, their composition, size and bandgap along with the photon-to-exciton QY found in each case at a given bandgap multiple and the MEG efficiency (η_{MEG}) for each sample.

PbS_xSe_{1-x} QDs, between 3 and 10 nm in diameter, as the size increases, η_{MEG} decreases linearly. For most sizes of PbS, MEG is less efficient than for PbSe QDs. These results are in agreement with recent comparison of MEG in PbS and PbSe QDs.[9] In that report, we measured the QYs at a fixed $h\nu$ for each QD-size, thus varying $h\nu/E_g$ by changing E_g rather than using multiple excitation wavelengths, thus the size-dependent η_{MEG} could not be determined. For similar confinement energies the QY is lower for PbS QDs compared to PbSe QDs despite similar Auger decay times suggestive of a similar strength of carrier−carrier interactions.[9] This points toward a possible difference in the rates of energy losses competing with MEG. Indeed, the analysis of carrier cooling due to polar coupling with longitudinal optical (LO) phonons indicates that the intraband relaxation rate in bulk PbSe is ca. twice as fast as in bulk PbS.[9] Further, the transition to a bulk-like intraband relaxation in PbS QDs likely occurs at smaller sizes than in PbSe QDs because PbS has a larger LO phonon energy, and therefore, relaxation via single-phonon processes becomes possible for larger confinement energies.

In their seminal paper on the electronic properties of QDs, Efros and Efros define a "smallness parameter" ($\lambda = r/a_B$) to describe the degree of quantum confinement[37] and identified the strong confinement regime when $r \ll a_B$ ($\lambda \ll 1$). In this regime, the motions of electrons and holes are strongly affected by the physical dimension of the system. The Bohr exciton radius for PbS is 18−20 nm compared to 46 nm for PbSe. For a pictorial comparison we show in Figure 4d a circle with the Bohr radius of PbSe and PbS compared to a QD with diameter of 10 nm. The Bohr exciton radius, a_B, is a measure of the characteristic distance between a bound electron and hole in a bulk semiconductor.[38] Excitons in bulk semiconductors are bound by the Coulomb force giving rise to a Rydberg energy series below the free-electron continuum of the conduction band. These bulk excitons only exist at low temperatures where $k_BT < E_{Ry}$ and under conditions where no excess energy is applied to the system.

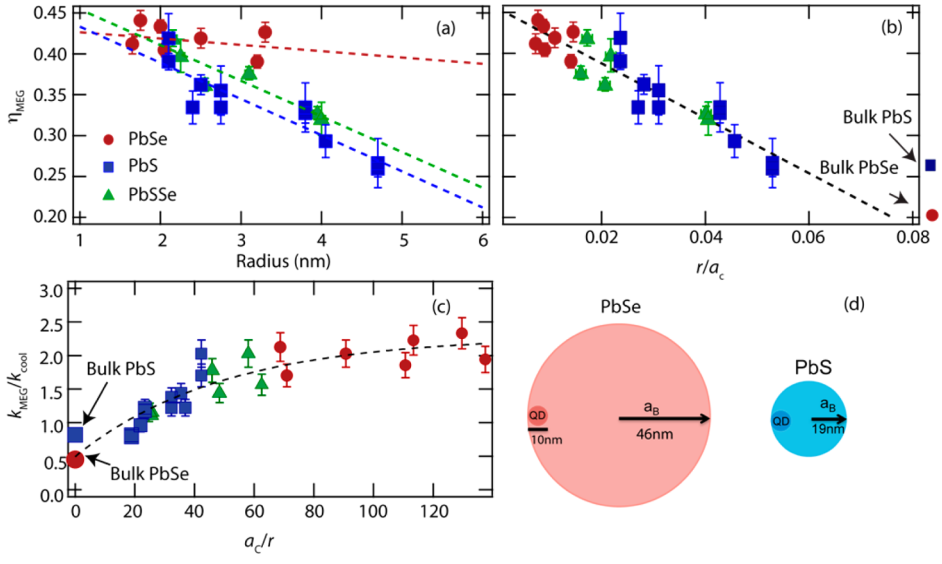

Figure 4. (a) MEG efficiency plotted verses QD size for PbS, PbSe, and PbS_xSe_{1-x}. (b) MEG efficiency plotted vs the QD-radius divided by the characteristic radius, a_C, where Coulomb binding energy equals the confinement energy. (c) The parameter P (competition between MEG rate and cooling rate) is plotted verses a_c/r. The efficiency of bulk PbS and PbSe are shown at $a_c/r = 0$. Panel (d) illustrates the difference in the Bohr radius for QDs (diameter 10 nm) of PbSe and PbS.

dx.doi.org/10.1021/nl4009748 | Nano Lett. 2013, 13, 3078−3085

The spatial extent of excitons in strongly confined QDs is defined not by the Coulomb force but by the dimensions of the nanocrystal. Therefore, the energies of quantized levels are dictated primarily by confinement while the e-h Coulomb attraction provides a relatively small correction. To define a critical QD size (a_c) for the onset of the strong confinement regime one can use an "energetic criterion", that is, a_c corresponds to the QD radius for which the Coulomb e-h binding energy ($e^2/\varepsilon a_c$) equals the confinement energy ($\pi^2\hbar^2/2m^*a_c^2$). On the basis of this criterion $a_c = \pi^2\hbar^2\varepsilon_\infty/2m^*e^2$, where ε_∞ is the high-frequency dielectric constant of the material and m^* is the reduced effective mass of the exciton $1/m^* = 1/m_e^* + 1/m_h^*$.

When η_{MEG} for PbSe, PbS, and PbS_xSe_{1-x} is plotted versus r/a_c (Figure 4b) the values fall along a line (black dotted line in Figure 4b); a_c for the alloyed QDs is a weighted reciprocal average. The linear behavior of η_{MEG} is likely a result of various competing processes that have QD-size dependence. As the QD-size increases to sizes larger than a_c, η_{MEG} should approach the impact ionization (II) efficiency found in the parent bulk semiconductor. At some large size, quantum confinement effects are reduced and a colloidal nanocrystal becomes a small piece of bulk material and the electronic and optical properties will follow suit. We show values of η_{MEG} for bulk PbS and PbSe to the right of Figure 4b; it is clear that the linear dependence on r/a_c observed for the QDs must break down at some point as the largest PbS QDs displayed an MEG efficiency equal to that of bulk PbS. The linear dependence is likely at least partially dependent on extrinsic effects such as imperfect surfaces, electronic effects associated with nonstoichiometry and increased cooling due to coupling to surface ligands. Measuring the QYs for larger PbS and PbSe QDs is experimentally challenging because larger QDs tend to precipitate from solution and the photon fluence needed to only excite one electron−hole pair becomes increasingly small. In order to display the values obtained previously for bulk PbSe and PbS together with the QD results, we replot the values of P as a function of the inverse of the a_c/r ratio (in Figure 4c); the value for bulk PbSe and PbS are shown at $a_c/r = 0$. We find that at smaller sizes, P saturates at a value of ~2.3. On the other hand, as the size increases, P decreases toward the bulk value of ~0.5. It is interesting that the results of the measurements seem to extrapolate better to the value of bulk PbSe rather than bulk PbS. The reason for this is unclear but could result from the fact that the available literature data[23] overestimate the impact ionization efficiency in bulk PbS. For example, previous MEG studies of refs 8 and 9 as well as the present work indicate that for a given $h\nu/E_g$ the MEG efficiency is systematically higher in PbSe QDs than in PbS QDs, while the measurements of ref [23] of bulk PbSe and PbS films indicate the opposite trend. This discrepancy highlights the need for a new independent assessment of MEG yields in bulk PbS and PbSe.

There are several theoretical descriptions of the MEG process that have primarily dealt with how k_{MEG} depends upon quantum confinement and neglect the size-dependence of k_{cool}.[36,39−41] These studies attempt to predict the size-dependence of MEG. Rabani et al. studied small QDs of CdSe, InAs, and Si and showed that as the QD size increased, k_{MEG} decreased.[39,42] Lin et al. expanded on this work by examining larger QDs of CdSe, including spin−orbit coupling and excitonic interactions in order to calculate k_{MEG}; they also specifically addressed the issue of size scaling.[36] Their conclusions are in agreement with results of Rabani et al. in that k_{MEG} is found to depend on the volume of the QD, with larger sizes leading to a slower MEG. In both treatments, this size-dependent MEG is attributed to a competition between the Coulomb coupling (matrix element W_c) and the density of trion states, ρ_f. In the Fermi-Golden rule approximation, k_{MEG} is expressed as a product of $|W_c|^2$ and ρ_f:[8,42]

$$k_{MEG} = \left(\frac{2\pi}{\hbar}\right)|W_c|^2\rho_f \tag{3}$$

The increase in the biexciton density of states, ρ_{xx} with increasing excess energy far exceeds the increase in ρ_x (ρ_{xx} is zero for excess energies less than $2E_g$)[43] and the excess energy at which ρ_{xx} surpasses ρ_x is generally regarded as the onset energy for MEG.[44] W_c decreases with increasing QD size (but is constant with increasing excitation energy) while ρ_{xx} increases with increasing size and increasing excess energy. The volume dependence of W_c and ρ_f leads to an overall increase in the MEG rate with decreasing size. Lin et al. conclude that k_{MEG} approximately has a V^{-1} dependence,[36] which is similar to the dependence observed for the Auger recombination rate.[45,46] Our measurements indicate that the overall MEG efficiency has a diameter dependence rather than volume dependence. The difference between theory and experiment may be due to a diameter-dependent cooling rate; the cooling rate would need to increase as the diameter decreases with a d^{-2} dependence. A fast increase in the intraband relaxation rate with decreasing QD size was previously observed for both CdSe[47,48] and PbSe[49] nanocrystals. These trends are opposite to the expected slower exciton cooling rate predicted by the phonon-bottleneck, where it is hypothesized that the wider spacing between quantized energy levels at smaller QD sizes requires greater numbers of simultaneous multiphonon−electron scattering events which become increasingly difficult. Exciton cooling rates in quantum-confined nanocrystals is still an active area of research. Evidence for significantly slower hot exciton cooling QDs relative to hot carrier cooling in bulk semiconductors is rather strong,[50−52] but a complete picture of the different cooling pathways, in particular, how and when the phonon-bottleneck is bypassed in quantized semiconductors has not been worked out.[50] MEG is an efficient cooling mechanism and when available (hot-exciton has sufficient excess energy) competes favorably with other loss mechanisms.

Conclusion. We report η_{MEG} for PbS and PbS_xSe_{1-x} alloy QD samples over a wide range of sizes and compositions and compare those results to previous measurements on PbSe QDs. We find that unlike the PbSe QD samples, there is a dependence of MEG on QD radius in PbS QDs as well as the alloyed samples. Furthermore, when the QD radius is normalized by a material-dependent characteristic radius, defined as the radius where the Coulomb and quantum confined energies are equal, the η_{MEG} for PbS, PbSe, and their alloys all fall on the same trend line with an increasing η_{MEG} for smaller normalized radii. The competition between k_{MEG} and k_{cool} favors MEG for smaller sizes. Theoretical treatments predict an increase in k_{MEG} with decreasing size that varies approximately with inverse QD volume. The exciton cooling rate constant, k_{cool}, also likely increases with decreasing volume but with a dependence that is weaker than for k_{MEG} resulting in the linear increase of the MEG yield with decreasing r; the size-dependence of the hot exciton cooling in nanocrystals is not well understood. These results taken with current theoretical models of MEG suggest that higher η_{MEG} could be achieved if

dx.doi.org/10.1021/nl4009748 | Nano Lett. 2013, 13, 3078−3085

some degree of control of the carrier cooling dynamics could be achieved. A promising recent study found η_{MEG} to be enhanced in PbSe nanorods with moderate aspect ratios compared to QDs.[25,26] It was suggested that this increase resulted primarily from an increase in k_{MEG} as recent measurements of intraband relaxation in PbSe nanorods[53] indicated that carrier cooling rates were not significantly affected by elongation of the nanocrystal.

Methods. PbS QDs were synthesized according to the typical hot injection method following ref 54 PbS_xSe_{1-x} alloy samples were synthesized according ref 55 percentages of sulfur and selenium were determined using inductivity coupled plasma atomic emission spectroscopy (ICP-AES) and verified by shifts in X-ray diffraction peaks. A similar preparation was determined to produce high quality alloys using Rutherford backscattering spectroscopy and energy filtered TEM.[56] The sizes of the alloy QDs are calculated by using the sizing curves of PbS and PbSe and assuming Vegard's law and were verified by direct observation with transmission electron microscopy (TEM).[55] For spectroscopic measurements, samples were dispersed in organic solvents (e.g., hexane or tetrachloroethylene) and loaded into airtight cuvettes under inert atmosphere in a glovebox. Special care was taken to avoid photocharging by stirring samples during the measurements.[4,15,16] Photocharging has been shown to lead to the overestimation of the MEG efficiency due to slow accumulation of charged nanocrystals within the excitation volume resulting in the development of "parasitic" contributions to the apparent MEG signal due to Auger recombination of charged excitations (e.g., trions and charged biexcitons).

MEG yields were determined using ultrafast transient absorption (TA) spectroscopy and transient photoluminescence (PL) measurements employing PL up-conversion (uPL). The experimental setups are described in detail in refs 4 and 57. Briefly, in order to determine the photon-to-exciton quantum yields (QYs) via TA measurements, the first exciton bleach dynamics for a variety of excitation fluences are measured with a temporal resolution of ~100 fs and the transients are collected until a pump−probe delay time of at least 3 times the biexciton lifetime. From these transients, the ratio of the transient bleach (reduction of interband absorption) at early pump−probe delay times to the respective signal at long pump−probe delay times was extracted. The bleach at early pump−probe delays is proportional to the number of excitons per QD produced by the laser pulse while at long delay times it is proportional to the total number of the nanocrystals excited by the laser pulse, as all multiexcitons have decayed to produce signal excitons. We label the ratio of the transient bleach at early times (a) to late times (b) as $R_{pop} = a/b$. In the case of weak 1S bleaching (no saturation of the 1S state), this ratio provides a direct measured of exciton multiplicity, which in the limit of $N_0 \rightarrow 0$ represents the QE of photon-to-exciton conversion.[1,57,58]

We correct for any decay in the single excitons over this time by comparing the R_{pop} value found below the MEG threshold to the R_{pop} above the MEG threshold. We find that by reducing the photon fluence of the excitation pulse so that $N_0 < 0.1$ while stirring, we are able to extract the correct photon-to-exciton QY, while reducing the contribution from photocharging. If $R_{pop} > 1$ for these low photon fluences, single photons absorbed in a QD must have created multiple excitons. For each of the samples studied, a set of TA traces was taken below $2E_g$ and at least one set was taken above $3E_g$ in order to determine the MEG efficiency.

Similar procedures for extracting QE were applied in the case of uPL measurements. However, due to a quadratic scaling of the PL signal with QD excitonic occupancy, the QE was derived from the following expression: $QE = (A/B + 2)/3$, where A and B are early and late-time PL amplitudes, respectively, measured in the limit of $N_0 \rightarrow 0$.[4,15]

AUTHOR INFORMATION

Corresponding Author

*E-mail: matt.beard@nrel.gov.

Notes

The authors declare no competing financial interest.

ACKNOWLEDGMENTS

A.G.M and M.C.B acknowledge support from the Solar Photochemistry program within the division of Chemical Sciences, Geosciences, and Biosciences, Office of Science, Office of Basic Energy Sciences (BES) funded by the Department of Energy (DOE). J.M.L, J.T.S, D.K.S, L.A.P, V.I.K, and A.J.N were supported as part of the Center for Advanced Photophysics (CASP) an Energy Frontier Research Center (EFRC) funded by BES.

REFERENCES

(1) Schaller, R.; Klimov, V. High Efficiency Carrier Multiplication in PbSe Nanocrystals: Implications for Solar Energy Conversion. *Phys. Rev. Lett.* **2004**, *92*, 186601.

(2) Ellingson, R. J.; Beard, M. C.; Johnson, J. C.; Yu, P.; Micic, O. I.; Nozik, A. J.; Shabaev, A.; Efros, A. L. Highly Efficient Multiple Exciton Generation in Colloidal PbSe and PbS Quantum Dots. *Nano Lett.* **2005**, *5*, 865.

(3) Nair, G.; Geyer, S. M.; Chang, L. Y.; Bawendi, M. G. Carrier multiplication yields in PbS and PbSe nanocrystals measured by transient photoluminescence. *Phys. Rev. B* **2008**, *78*, 10.

(4) McGuire, J. A.; Joo, J.; Pietryga, J. M.; Schaller, R. D.; Klimov, V. I. New Aspects of Carrier Multiplication in Semiconductor Nanocrystals. *Acc. Chem. Res.* **2008**, *41*, 1810−1819.

(5) Beard, M. C.; Midgett, A. G.; Hanna, M. C.; Luther, J. M.; Hughes, B. K.; Nozik, A. J. Comparing Multiple Exciton Generation in Quantum Dots To Impact Ionization in Bulk Semiconductors: Implications for Enhancement of Solar Energy Conversion. *Nano Lett.* **2010**, *10*, 3019−3027.

(6) Trinh, M. T.; Houtepen, A. J.; Schins, J. M.; Hanrath, T.; Piris, J.; Knulst, W.; Goossens, A.; Siebbeles, L. D. A. In spite of recent doubts carrier multiplication does occur in PbSe nanocrystals. *Nano Lett.* **2008**, *8*, 1713−1718.

(7) Ji, M.; Park, S.; Conner, S. T.; Mokari, T.; Cui, Y.; Gaffney, K. J. Efficient Mulitple Exciton Generation Observed in Colloidal PbSe Quantum Dots with Temporally and Spectrally Resolved Intraband Excitation. *Nano Lett.* **2009**, *9*, 1217−1222.

(8) Trinh, M. T.; Polak, L.; Schins, J. M.; Houtepen, A. J.; Vaxenburg, R.; Maikov, G. I.; Grinbom, G.; Midgett, A. G.; Luther, J. M.; Beard, M. C.; Nozik, A. J.; Bonn, M.; Lifshitz, E.; Siebbeles, L. D. A. Anomalous Independence of Multiple Exciton Generation on Different Group IV-VI Quantum Dot Architectures. *Nano Lett.* **2011**, *11*, 1623−1629.

(9) Stewart, J. T.; Padilha, L. A.; Qazilbash, M. M.; Pietryga, J. M.; Midgett, A. G.; Luther, J. M.; Beard, M. C.; Nozik, A. J.; Klimov, V. I. Comparison of Carrier Multiplication Yields in PbS and PbSe Nanocrystals: The Role of Competing Energy-Loss Processes. *Nano Lett.* **2012**, *12*, 622−628.

(10) Wise, F. W. Lead Salt Quantum Dots: the Limit of Strong Quantum Confinement. *Acc. Chem. Res.* **2000**, *33*, 773.

(11) Rogach, A. L.; Eychmuller, A.; Hickey, S. G.; Kershaw, S. V. Infrared-emitting colloidal nanocrystals: Synthesis, assembly, spectroscopy, and applications. *Small* **2007**, *3*, 536−557.
(12) Wadia, C.; Alivisatos, A. P.; Kammen, D. M. Materials Availability Expands the Opportunity for Large-Scale Photovoltaics Deployment. *Environ. Sci. Technol.* **2009**, *43*, 2072−2077.
(13) Nozik, A. J.; Beard, M. C.; Luther, J. M.; Law, M.; Ellingson, R. J.; Johnson, J. C. Semiconductor Quantum Dots and Quantum Dot Arrays and Applications of Multiple Exciton Generation to Third-Generation Photovoltaic Solar Cells. *Chem. Rev.* **2010**, *110*, 6873−6890.
(14) Semonin, O. E.; Luther, J. M.; Choi, S.; Chen, H. Y.; Gao, J. B.; Nozik, A. J.; Beard, M. C. Peak External Photocurrent Quantum Efficiency Exceeding 100% via MEG in a Quantum Dot Solar Cell. *Science* **2011**, *334*, 1530−1533.
(15) McGuire, J. A.; Sykora, M.; Joo, J.; Pietryga, J. M.; Klimov, V. I. Apparent Versus True Carrier Multiplication Yields in Semiconductor Nanocrystals. *Nano Lett.* **2010**, *10*, 2049−2057.
(16) Midgett, A. G.; Hillhouse, H. W.; Huges, B. K.; Nozik, A. J.; Beard, M. C. Flowing versus Static Conditions for Measuring Multiple Exciton Generation in PbSe Quantum Dots. *J. Phys. Chem. C* **2010**, *114*, 17486−17500.
(17) Sambur, J. B.; Novet, T.; Parkinson, B. A. Multiple Exciton Collection in a Sensitized Photovoltaic System. *Science* **2010**, *330*, 63−66.
(18) Kim, S. J.; Kim, W. J.; Sahoo, Y.; Cartwright, A. N.; Prasad, P. N. Multiple exciton generation and electrical extraction from a PbSe quantum dot photoconductor. *Appl. Phys. Lett.* **2008**, *92*, 3.
(19) Sukhovatkin, V.; Hinds, S.; Brzozowski, L.; Sargent, E. H. Colloidal Quantum-Dot Photodetectors Exploiting Multiexciton Generation. *Science* **2009**, *324*, 1542−1544.
(20) Gdor, I.; Sachs, H.; Roitblat, A.; Strasfeld, D. B.; Bawendi, M. G.; Ruhman, S. Exploring Exciton Relaxation and Multiexciton Generation in PbSe Nanocrystals Using Hyperspectral Near-IR Probing. *ACS Nano* **2012**, *6* (4), 3269−3277.
(21) Aerts, M.; Sandeep, C. S. S.; Gao, Y. A.; Savenije, T. J.; Schins, J. M.; Houtepen, A. J.; Kinge, S.; Siebbeles, L. D. A. Free Charges Produced by Carrier Multiplication in Strongly Coupled PbSe Quantum Dot Films. *Nano Lett.* **2011**, *11*, 4485−4489.
(22) Nair, G.; Chang, L. Y.; Geyer, S. M.; Bawendi, M. G. Perspective on the Prospects of a Carrier Multiplication Nanocrystal Solar Cell. *Nano Lett.* **2011**, *11*, 2145−2151.
(23) Pijpers, J. J. H.; Ulbricht, R.; Tielrooij, K. J.; Osherov, A.; Golan, Y.; Delerue, C.; Allan, G.; Bonn, M. Assessment of carrier-multiplication efficiency in bulk PbSe and PbS. *Nat. Phys.* **2009**, *5*, 811−814.
(24) Alig, R. C.; Bloom, S. Electron-Hole-Pair Creation Energies in Semiconductors. *Phys. Rev. Lett.* **1975**, *35*, 1522.
(25) Sandberg, R. L.; Padilha, L. A.; Qazilbash, M. M.; Bae, W. K.; Schaller, R. D.; Pietryga, J. M.; Stevens, M. J.; Baek, B.; Nam, S. W.; Klimov, V. I. Multiexciton Dynamics in Infrared-Emitting Colloidal Nanostructures Probed by a Superconducting Nanowire Single-Photon Detector. *ACS Nano* **2012**, *6*, 9532−9540.
(26) Padilha, L. A.; Stewart, J. T.; Sandberg, R. L.; Bae, W. K.; Koh, W. K.; Pietryga, J. M.; Klimov, V. I. Carrier Multiplication in Semiconductor Nanocrystals: Influence of Size, Shape and Composition. *Acc. Chem. Res.* **2013**, DOI: 10.1021/ar300228x.
(27) Beard, M. C.; Knutsen, K. P.; Yu, P. R.; Luther, J. M.; Song, Q.; Metzger, W. K.; Ellingson, R. J.; Nozik, A. J. Multiple exciton generation in colloidal silicon nanocrystals. *Nano Lett.* **2007**, *7*, 2506−2512.
(28) Trinh, M. T.; Limpens, R.; de Boer, W.; Schins, J. M.; Siebbeles, L. D. A.; Gregorkiewicz, T. Direct generation of multiple excitons in adjacent silicon nanocrystals revealed by induced absorption. *Nat. Photonics* **2012**, *6*, 316−321.
(29) Wang, S. J.; Khafizov, M.; Tu, X. M.; Zheng, M.; Krauss, T. D. Multiple Exciton Generation in Single-Walled Carbon Nanotubes. *Nano Lett.* **2010**, *10*, 2381−2386.
(30) Stubbs, S. K.; Hardman, S. J. O.; Graham, D. M.; Spencer, B. F.; Flavell, W. R.; Glarvey, P.; Masala, O.; Pickett, N. L.; Binks, D. J. Efficient carrier multiplication in InP nanoparticles. *Phys. Rev. B* **2010**, *81*, 081303.
(31) Bertazzi, F.; Moresco, M.; Penna, M.; Goano, M.; Bellotti, E. Full-Band Monte Carlo Simulation of HgCdTe APDs. *J. Electron. Mater.* **2010**, *39*, 912−917.
(32) Tirino, L.; Weber, M.; Brennan, K. F.; Bellotti, E.; Goano, M. Temperature dependence of the impact ionization coefficients in GaAs, cubic SiC, and zinc-blende GaN. *J. Appl. Phys.* **2003**, *94*, 423−430.
(33) Ziaja, B.; London, R. A.; Hajdu, J. Ionization by impact electrons in solids: Electron mean free path fitted over a wide energy range. *J. Appl. Phys.* **2006**, *99*, 9.
(34) Cho, B.; Peters, W. K.; Hill, R. J.; Courtney, T. L.; Jonas, D. M. Bulklike Hot Carrier Dynamics in Lead Sulfide Quantum Dots. *Nano Lett.* **2010**, *10*, 2498−2505.
(35) Ridley, B. K. Quantum Processes in Semiconductors, 2nd ed.; Oxford University Press: New York, 1988.
(36) Lin, Z. B.; Franceschetti, A.; Lusk, M. T. Size Dependence of the Multiple Exciton Generation Rate in CdSe Quantum Dots. *ACS Nano* **2011**, *5*, 2503−2511.
(37) Efros, A. L.; Efros, A. L. *Sov. Phys. Semicond* **1982**, *16*, 772.
(38) Kayanuma, Y. Wannier Exciton in Microcrystals. *Solid State Commun.* **1986**, *59*, 405−408.
(39) Rabani, E.; Baer, R. Theory of multiexciton generation in semiconductor nanocrystals. *Chem. Phys. Lett.* **2010**, *496*, 227−235.
(40) Rabani, E.; Baer, R. Distribution of Multiexciton Generation Rates in CdSe and InAs Nanocrystals. *Nano Lett* **2008**, *8*, 4488−4492.
(41) Witzel, W. M.; Shabaev, A.; Hellberg, C. S.; Jacobs, V. L.; Efros, A. L. Quantum Simulation of Multiple-Exciton Generation in a Nanocrystal by a Single Photon. *Phys. Rev. Lett.* **2010**, *105*, 137401.
(42) Baer, R.; Rabani, E. Expeditious Stochastic Calculation of Multiexciton Generation Rates in Semiconductor Nanocrystals. *Nano Lett.* **2012**, *12*, 2123−2128.
(43) Rupasov, V. I.; Klimov, V. I. Carrier multiplication in semiconductor nanocrystals via intraband optical transitions involving virtual biexciton states. *Phys. Rev. B* **2007**, *76*, 125321.
(44) Franceschetti, A.; An, J. M.; Zunger, A. Impact Ionization Can Explain Carrier Multiplication in PbSe Quantum Dots. *Nano Lett.* **2006**, *6*, 2191−2195.
(45) Klimov, V. I.; Mikhailovsky, A. A.; McBranch, D. W.; Leatherdale, C. A.; Bawendi, M. G. Quantization of Multiparticle Auger rates in Semiconductor Quantum Dots. *Science* **2000**, *287*, 1011−1013.
(46) Robel, I.; Gresback, R.; Kortshagen, U.; Schaller, R. D.; Klimov, V. I. Universal Size-Dependent Trend in Auger Recombination in Direct-Gap and Indirect-Gap Semiconductor Nanocrystals. *Phys. Rev. Lett.* **2009**, *102*, 177404.
(47) Klimov, V. I.; McBranch, D. W. Femtosecond 1P-to-1S Electron Relaxation in Strongly Confined Semiconductor Nanocrystals. *Phys. Rev. Lett.* **1998**, *80*, 4028−4031.
(48) Klimov, V. I.; McBranch, D. W.; Leatherdale, C. A.; Bawendi, M. G. Electron and Hole Relaxation Pathways in Semiconductor Quantum Dots. *Phys. Rev. B* **1999**, *60*, 13740−13749.
(49) Schaller, R. D.; Pietryga, J. M.; Goupalov, S. V.; Petruska, M. A.; Ivanov, S. A.; Klimov, V. I. Breaking the phonon bottleneck in semiconductor nanocrystals via multiphonon emission induced by intrinsic nonadiabatic interactions. *Phys. Rev. Lett.* **2005**, *95*, 196401.
(50) Nozik, A. J.. Quantum Structured Solar Cells. In *Nanostructured Materials for Solar Energy Conversion*; Soga, T., Ed.; Elsevier: New York, 2006; pp 485−516.
(51) Blackburn, J. L.; Ellingson, R. J.; Micic, O. I.; Nozik, A. J. Electron relaxation in colloidal InP quantum dots with photogenerated excitons or chemically injected electrons. *J. Phys. Chem. B* **2003**, *107*, 102−109.
(52) Pandey, A.; Guyot-Sionnest, P. Slow Electron Cooling in Colloidal Quantum Dots. *Science* **2008**, *322*, 929.

(53) Yang, J.; Hyun, B. R.; Basile, A. J.; Wise, F. W. Exciton Relaxation in PbSe Nanorods. *ACS Nano* **2012**, *6*, 8120−8127.
(54) Hines, M. A.; Scholes, G. D. Colloidal PbS nanocrystals with size-tunable near-infrared emission: Observation of post-synthesis self-narrowing of the particle size distribution. *Adv. Mater.* **2003**, *15*, 1844−1849.
(55) Smith, D. K.; Luther, J. M.; Semonin, O. E.; Nozik, A. J.; Beard, M. C. Tuning the Synthesis of Ternary Lead Chalcogenide Quantum Dots by Balancing Precursor Reactivity. *ACS Nano* **2011**, *5*, 183−190.
(56) Ma, W.; Luther, J. M.; Zheng, H.; Wu, Y.; Alivisatos, A. P. Photovoltaic Devices Employing Ternary PbS_xSe_{1-x} Nanocrystals. *Nano Lett.* **2009**, *9*, 1699−1703.
(57) Beard, M. C.; Ellingson, R. J. Multiple exciton generation in semiconductor nanocrystals: Toward efficient solar energy conversion. *Laser Photon. Rev.* **2008**, *2*, 377−399.
(58) Schaller, R. D.; Agranovitch, V. M.; Klimov, V. I. *Nat. Phys.* **2005**, *1*, 189.

dx.doi.org/10.1021/nl4009748 | *Nano Lett.* 2013, 13, 3078−3085